Direct Hydrocarbon Saturation Imaging in Porous Media with ^{13}C

Naser Ansaribaranghar[1,2], *Mohammad Sadegh* Zamiri[1], *Laura* Romero-Zerón[2], *Florea* Marica[1], *Andrés* Ramírez Aguilera[1], *Derrick* Green[4], *Benjamin* Nicot[3] and *Bruce J.* Balcom[1,*]

[1]UNB MRI Centre, Department of Physics, University of New Brunswick, Fredericton, New Brunswick E3B 5A3, Canada
[2]Department of Chemical Engineering, University of New Brunswick, Fredericton, New Brunswick E3B 5A3, Canada
[3]TotalEnergies, Avenue Larribau, 64000 Pau, France
[4]Green Imaging Technologies, Fredericton, New Brunswick E3A 8V2, Canada

Abstract. Executing a successful waterflood recovery project in the field requires prior laboratory core flooding studies in order to understand fluid displacement and predict the recovery efficiency. When dealing with reservoir rocks that display complex fluid distribution (for example due to pore size heterogeneity, capillary end effect, or wettability heterogeneity), the use of an imaging technique is crucial. Traditionally, fluid saturation changes during core floods are monitored using X-Rays. However, the use of dopants is usually required in order to improve the density contrast between fluids. These dopants may alter the wettability of the rock or could chemically inhibit some EOR operations, such as low salinity injection. In this work we introduce a simple Magnetic Resonance Imaging measurement to monitor hydrocarbon saturation profiles. This measurement, selective for hydrocarbons, requires no contrast agents or unusual fluids. We employ Carbon-13 measurements of carbon in the hydrocarbon phase to directly detect oil with natural abundance ^{13}C. This allows for spatial quantification of oil saturation in core plug samples. The core plugs tested were water-wet Berea and Bentheimer sandstones and oil-wet (treated) Bentheimer sandstones. Viscosity standard oils were used as the oil phase, and brine (2.1 wt% NaCl) was used as the water phase. Imaging was performed using the 1D Hybrid SE-SPI MRI method. The results showed that the ^{13}C 1D images provided high quality saturation information. Dean-Stark analysis on the final state of the core plugs confirmed the saturations. The ^{13}C bearing phase was directly observed, and there was no need for further processing to separate the signals. Flooding in different combinations of fluids, rocks, and wettability conditions was examined by 1D imaging. The ^{13}C profile method clearly reveals hydrocarbon capillary end effects in oil wet samples. The ability to generate direct ^{13}C profiles is a general capability which is applicable to a wide range of flooding experiments and core analysis measurements. In particular, it provides an alternative to the common use of D_2O in profile MRI studies to eliminate observation of the water phase. These studies are greatly facilitated by a variable field magnet which permits sequential measurement of ^{1}H and ^{13}C in the same magnet with the same RF probe.

1 Introduction

Obtaining accurate spatially resolved saturation measurements in multiphase systems is an important issue in Hydrogeology, Environmental, Chemical, and Petroleum Engineering. In particular, saturation distribution is crucial for relative permeability and capillary pressure measurements, and for assessing oil recovery methods [1–6].

The industry-standard method for monitoring saturation state during core flooding experiments is X-ray computed tomography (CT) scanning combined with effluent analysis. CT scanning has sufficient temporal and spatial resolution, but often requires the addition of doping agents to enhance the fluid-phase contrast. These doping agents alter fluid densities, and can influence chemical interactions and interfacial properties [7]. It also limits the analysis of smart water methods such as low salinity brine injection.

Magnetic Resonance is a noninvasive method which aids determination of many porous rock properties [8]. One dimensional ^{1}H and relaxation time (T_1, T_2) methods are widely used for saturation determinations [9–12]. Muir and Balcom [10] compared four magnetic resonance imaging methods for fluid content imaging in water-saturated reservoir core plugs: frequency-encoded spin echo, single point ramped imaging with T_1 enhancement, hybrid spin echo single point imaging (SE-SPI), and T_2 mapping SE-SPI. Olsen et al. [11] used 1D chemical shift imaging method in chalk core plug samples saturated with oil and water.

There are many challenges in realistic complex samples. Rauschhuber et al. [12] used 1D RARE and reported that with an echo spacing on the order of milliseconds, the RARE sequence would not accurately measure a sandstone's clay bound water. Dick et al. [9]

* Corresponding author: bjb@unb.ca

did 1D T_2 mapping, and reported that the accuracy of the saturation improved when the T_2 spectrum did not have overlapping water and oil T_2 peaks. In such samples there can be significant overlap in the T_2 distributions of different fluids when imbibed in the pores of a rock [7]. In this case the abovementioned methods are not helpful. So, a requirement of measurement is that the water and oil peaks are well resolved in T_2. Separation of the oil and water T_2 peaks depends on the magnetic field and type of oil. This overlapping of the spectral T_2 signals is worse as B_0 inhomogeneity increases [11].

To obtain oil saturation in cases where phase differentiation is difficult, two main approaches are described in the literature. In the first approach, D_2O is used as the water phase, then ^1H profiles are representative of the oil phase. In the second approach fluorinated oil is used to distinguish water from oil, so that a qualitative distribution of oil saturation can be obtained by comparing the difference in the MR T_2 spectrum before and after coreflooding experiments [13].

Bulk and spatially resolved two dimensional methods such as T_1-T_2 or D-T_2 are also useful for distinguishing signals from different phases [7,12,14,15]. Rauschhuber et al. reported that D-T_2 experiments are insensitive to both the clay bound and irreducible capillary bound water. Although these techniques are valuable, they suffer from being time consuming, or needing models and assumptions for distinguishing overlapping signals. Mitchell et al. [7] reported that prior knowledge of the relaxation and diffusion properties of the liquids should be utilized to optimize the data acquisition to return a quantitative measure of the saturation state.

The goal of this study is to use natural abundance ^{13}C for MRI measurements inside porous media. ^{13}C nuclei exist in the hydrocarbon phase. MR profiles obtained in this way are solely from the hydrocarbon or ^{13}C bearing fluids. Chen et al. [6] showed the application of ^{13}C MRI to monitor saturation profiles of a commercial oil injected into a sand bed. In their experiments, they used an oil with short T_1 to obtain saturation profiles in a reasonable time during the flooding experiments. In this paper two sets of experiments were performed to test the ^{13}C application in obtaining oil saturation profiles. One set is dedicated to exploring end point saturation profiles of the samples at different wettability while the other set of experiments deals with coreflood monitoring of two sandstones. To generalize the application of ^{13}C MRI, an oil sample with a relatively long T_1 was selected.

By preparing samples with different wettability conditions and saturating them with different saturation histories, ^{13}C profiles revealed information on capillary end effects and residual/irreducible saturations which are very challenging to determine in flooding experiments and relative permeability calculations.

Capillary end effects arise from the discontinuity of capillarity in the wetting phase at the outlet end of the core sample. The capillary end effect is an important issue in coreflooding experiments because it can cause serious errors in the calculation of saturation and relative permeabilities from pressure drop and production information [16,17]. In-situ saturation monitoring can address this problem, but the option may not be available for every sample because of overlap of the T_2 distributions.

In this paper ^{13}C measurements are shown to be a reliable method to obtain spatially resolved hydrocarbon saturation which can be used to evaluate capillary end effects, residual oil saturation and irreducible water saturation.

2 Materials and Methods

The study was conducted in the form of a series of experiments on core plugs, with data being gathered via MR/MRI.

Rock and fluid properties. The brine solution was prepared using 2.1 wt% NaCl in distilled water. Viscosity standard oils (S6 and S20) were a product of CANNON Instrument Company (State College, PA, United States). Core plugs were cut and trimmed to the preferred dimensions (Table 1). Two core plugs (F1 and F2) were used in continuous flooding experiments. Samples F1 and F2 were Bentheimer and Berea sandstone core plugs respectively, initially saturated with brine. Then S20 oil was injected at different flow rates. The other core plugs in Table 1 were used to compare treated and untreated saturation states. Two of the samples, C1 and C2, were treated with the procedure mentioned below. Core plug C1 was vacuum saturated using brine while core plug C2 was vacuum saturated using S6 oil. Core plugs C3 and C4 were untreated core plugs vacuum saturated with S6 oil and brine respectively. After MR measurements, sample C4 was flooded with S6 oil while samples C2 and C3 were flooded with brine (each with 10 pore volume and injection rate of 2 cc/min and maximum injection rate of 5 cc/min).

Treatment. The following procedure [18] was used for treatment of the core plugs using AquaSil™ (Thermo Fisher Scientific, US): Core plugs were dried at 90 °C for 24 hours. Samples were then flooded using methanol to remove additional salts. Samples were subsequently dried for 24 hours at 100 °C. The two samples were vacuum saturated for 2 hours with the 11 wt% AquaSil solution (38.72 gr AquaSil). These two samples were flooded with 10 pore volumes of methanol to remove extra solution then dried for 24 hours at 100 °C to cure the surface.

MR measurements. ^{13}C and ^1H MR experiments were undertaken to obtain T_2, and T_1 as well as 1D images. 1D ^{13}C profiles were acquired with the Hybrid SE-SPI method which is a phase-encode MRI technique. Hybrid SE-SPI was used because of its sensitivity. Details of the Hybrid SE-SPI measurement can be found elsewhere [10,19]. The pulse sequence begins with a 90° pulse, followed by a series of 180° pulses interspersed with phase-encoding gradients of equal strength but opposite sign. After a period of $5 \times T_1$, the second half of k-space is collected by employing gradients that are of opposite sign, as illustrated in Figure 1. The two sides of k-space are combined, and the k = 0 point is averaged prior to Fourier transformation. The signal intensity of a Hybrid SE-SPI image is given by (1):

$$S = M_0 \quad (1)$$

Table 1. Core plugs dimensions and mass.

Core #	Fluid	Formation	Treatment condition	Length (mm)	Diameter (mm)	Dry mass (g)	Saturated mass (g)	Porosity (v/v)
F1	S20	BA	Untreated	52.8	37.9	125.4	137.4	0.20
F2	S20	BH	Untreated	51.6	3.80	115.0	128.7	0.23
C1	Brine	BH	Treated	29.6	37.6	65.8	73.9	0.25
C2	S6	BH	Treated	28.4	37.9	62.3	68.9	0.23
C3	S6	BH	Untreated	29.0	38.0	64.1	70.9	0.23
C4	Brine	BH	Untreated	30.2	38.0	68.9	76.7	0.23

where M_0 is the equilibrium magnetization. The k = 0 point is assumed to be acquired promptly after the initial 90° pulse, minimizing T_2 attenuation, so the signal is directly proportional to the magnetization and thereby the ^{13}C density.

1D ^1H profiles were acquired with the T_2 mapping SE-SPI method which is a pure phase-encode MRI technique for T_2 distribution mapping. Details of the T_2 mapping SE-SPI measurement can be found elsewhere [20–22].

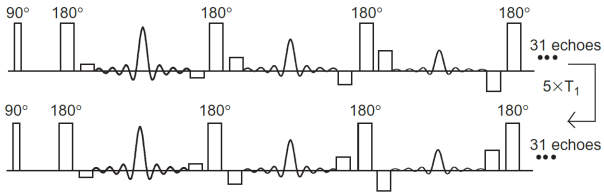

Fig. 1. Hybrid SE-SPI pulse sequence [10].

MR instruments. ^{13}C measurements were acquired using a variable field magnet (MR Solutions, Guildford, Surrey, UK) at 3.1 T with a resonance frequency of 33.7 MHz for ^{13}C. The RF probe was a homemade birdcage. The 3D gradient coil was driven by gradient amplifiers (Performance Controls, Inc., PA, US), providing maximum gradient strengths of 66.4 G/cm, 64.9 G/cm and 87.8 G/cm in the x, y and z directions. The magnet is permanently connected to a magnet power supply (Cryomagnetics, Inc., TN, US). GIT system software (Green Imaging Technologies, Inc., NB, Canada) was employed to execute CPMG and 1D Hybrid SE-SPI measurements.

All ^1H MR/MRI measurements were performed on a Maran DRX-HF (Oxford Instruments Ltd, Oxford, UK) 0.2 T permanent magnet which has a resonance frequency of 8.5 MHz for ^1H. The RF probe was a custom-built solenoid, 4.4 cm inner diameter, driven by a 1 kW 3445 RF amplifier (TOMCO Technologies, Sydney, Australia). A shielded three axis gradient coil driven by Techron (Elkhart, IN) 7782 gradient amplifiers, provided maximum magnetic field gradients of 26 G/cm^{-1}, 24 G/cm^{-1} and 33 G/cm^{-1} in x, y, and z, respectively.

Processing. To obtain ^{13}C 1D saturation images, the average of the highest signal amplitudes in cases with 100 % oil saturated core plugs were calculated and then profiles of the flooding experiments were scaled based on the fully saturated core plugs. This was done for samples C2 and C3, the samples that were initially 100 % oil saturated. Identical fully oil saturated core plugs were used for calibrating samples F1 and F2. We employed a Blackman filter in k-space to remove truncation artifacts in the images [23].

By assuming similar rock properties, the average highest signal of sample C3 was used for calibrating profiles of sample C4.

Fully oil saturated core plugs and bulk oil were employed as reference samples. By knowing the mass of the oil in the reference sample, a calibration value (gram/signal) could be obtained. After flooding, the signal amplitude of the CPMG experiments was multiplied by the calibration value and mass of the oil inside the core plug was obtained. Dividing the mass in the final state by the initial mass of the oil inside the sample (100 % oil saturated) results in oil saturation of the final state in the sample.

Flooding. A homemade low-pressure core holder was used for coreflooding. An ISCO pump was used for injecting the fluids. For the F1 sample, the injection rate started at 0.015 cc/min followed by 0.05, 0.1 and 0.5 cc/min injection rates. For the F2 sample, the injection rate started at 0.015 cc/min followed by 0.05, 0.1, 0.5 and 1 cc/min injection rates.

3 Results and Discussion

3.1. Calibration

To generate a quantitative measure of the saturation, it was necessary to first obtain a calibrated MR signal amplitude (arbitrary units), per unit mass of liquid. Using fully oil saturated core plugs, calibrated amplitudes were obtained for the oil phase. Each profile was then converted into 1D saturation images with the calibration sample. For bulk CPMG data signal per unit mass of the oil was calculated for the reference sample and then signal of the ^{13}C for the samples was converted to the oil saturation using this calibration number.

3.2. Static samples

^1H and ^{13}C profile and T_2 relaxation time measurements of three core plugs are presented. The first sample is an untreated core plug which was initially saturated with S6 oil and was flooded with brine. The second sample is a treated core plug which was initially saturated with S6 oil

Table 2. Parameters used for each instrument.

Experiment/Parameter	^{13}C (Variable field magnet) -Continuous flooding	^{13}C (Variable field magnet) -static measurements	^{1}H (8.5 MHz magnet)	
			Brine	oil
Instrument				
90° pulse duration (µs)	42.3	29.1	10.3	
180° pulse duration (µs)	85.9	60.7	20.5	
Frequency (MHz)	33.7	33.7	8.5	
CPMG				
Relaxation delay (Sec)	7.5	1.5	10	5
Echo time (ms)	1	4	2	1
Number of echoes collected	1000	375	2000	
Number of points collected at each echo	9	21	9	
Number of scans	32	256	32	
Digital filter (kHz)	200	50	125	
Hybrid SE-SPI profile (^{13}C)/T_2 Mapping SE-SPI (^{1}H)				
Relaxation delay (Sec)	7.5	1.5	$5\times T_1 = 5$	$5\times T_1 = 2.5$
Number of scans	128	256	4	
Resolution	64	64	64	
Field of view (cm)	10	8	8	
Echo time (ms)	5	5	2	
First Tau (µs)	-	-	1500	
Number of echoes collected	-	-	1024	
Number of points collected at each echo	9	9	9	
Dwell time (µs)	5	20	8	
Gradient	Min. gradient settling time (µs): 1500	Min. gradient settling time (µs): 1000	Ramp up (D1): 200 µs, Ramp down (D3): 200 µs, encoding time (D2): 300 µs	

and was flooded with brine. The third sample is an untreated core plug initially saturated with brine and flooded with S6 oil.

3.2.1 Brine saturated untreated core plug with residual oil (Sample # C3 flooded with brine)

Figure 2 shows a ^{13}C 1D image of the untreated Bentheimer core plug which was initially saturated with S6 and then flooded with brine. After 10 PV brine injection at left side, an even hydrocarbon distribution was observed, which corresponds to a uniform residual oil saturation of 27 %. As Figure 2 shows, no capillary end effect was observed. The sample was water wet and it was initially saturated with oil. A capillary end effect was not anticipated in this experiment. Bulk saturation obtained with CPMG data results in an oil saturation of 26.1 %. This value is very close to the saturation obtained from the ^{13}C profile.

Signals from oil and water phases were not distinguishable with ^{1}H measurements. The ^{1}H profile obtained from T_2 mapping SE-SPI (Figure 3) reveals no information regarding phases. The T_2 distribution (Figure 4) does not distinguish the two phases.

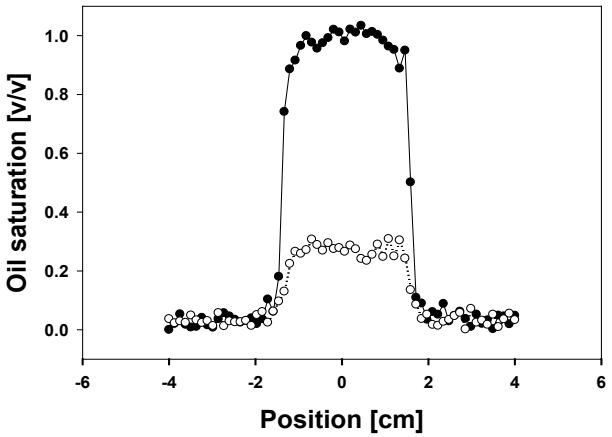

Fig. 2. ^{13}C Hybrid SE-SPI saturation profiles for untreated Bentheimer core plug saturated with brine with residual S6 oil. • is the spatially resolved signal (fully S6 saturated). ○ corresponds to the ^{13}C image of the sample after 10 PV of brine injection.

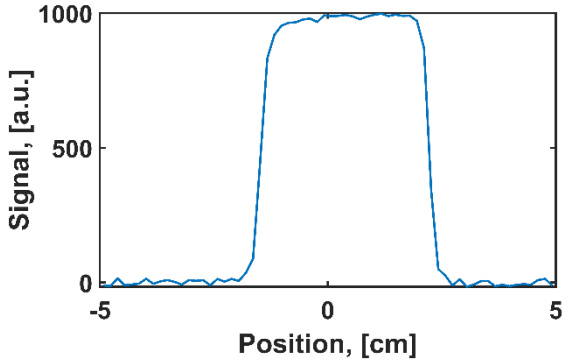

Fig. 3. ^{1}H T_2 mapping SE-SPI profile for untreated Bentheimer core plug saturated with brine and residual S6 oil.

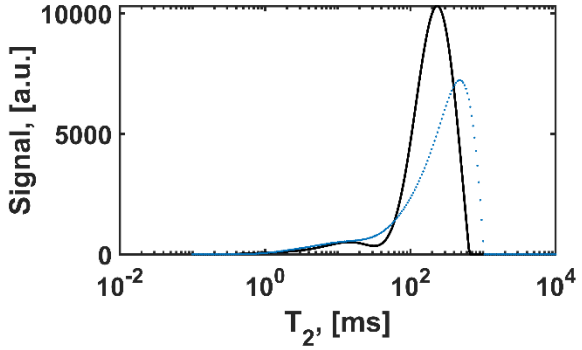

Fig. 4. ^{1}H T_2 distribution for untreated Bentheimer core plug saturated with brine and residual S6 oil. (.....) corresponds to the final state (S_{or}) while (——) corresponds to the initial state (fully oil saturated).

3.2.2 Brine saturated treated core plug with residual S6 (Sample # C2 flooded with brine)

Figure 5 shows a ^{13}C 1D image of the treated Bentheimer core plug at multiple time points. Initially the sample was saturated with S6 and then brine was injected (right side). After 10 PV injection of brine, the saturation image of the sample was heterogeneous. Saturation at the end of the sample (left) is higher than the other regions. This clearly shows a capillary end effect for the hydrocarbon which maintains a higher wetting phase (oil) saturation at the outlet.

After 10 PV brine injection, the oil saturation was 39% in the first half of the core plug (inlet). At the outlet of the core plug the residual oil saturation was 62%, which is due to capillary end effects.

When the sample was fully oil saturated the bulk CPMG signal amplitude was 99.78 a.u. for 6.53 gr of S6 inside the core plug. The signal amplitude was 88.66 a.u. after a half PV of brine injection. Comparing this value with the fully saturated case, results in 5.8 gr of S6 which means the oil saturation was 88.8%. This value is very close to the saturation obtained from the ^{13}C profile. The signal amplitude was 41.88 a.u. after 10 PV brine injection. Comparing this value with the fully saturated case, results in 2.74 gr of S6 which means the oil saturation was 41.9%. This value is 2-3% more than the oil saturation obtained from the ^{13}C profile (S_o=39%).

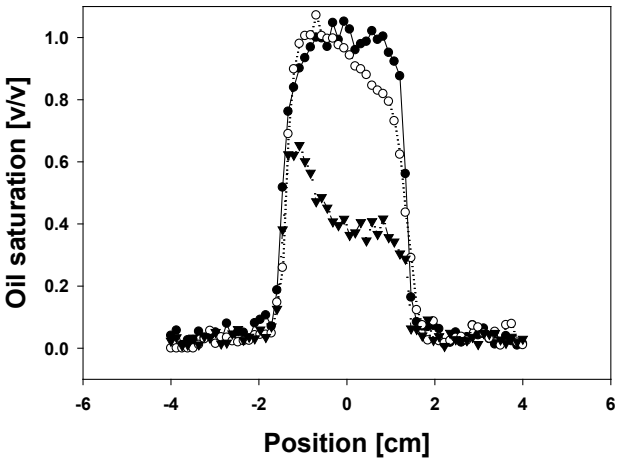

Fig. 5. ^{13}C Hybrid SE-SPI saturation profile for treated Bentheimer core plug saturated with brine with small amount of S6. • is related to the sample at initial state (fully S6 saturated). ○ is related to the profile of the sample after 5 cc of brine injection. ▼ shows the profile of the sample after 10 PV of brine injection. Injection was at the right of the core plug.

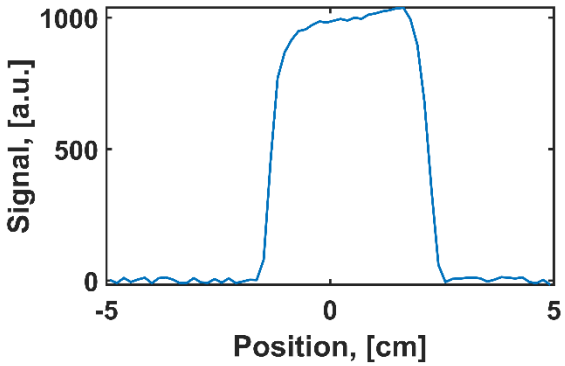

Fig. 6. ^{1}H T_2 mapping SE-SPI profile for treated Bentheimer core plug saturated with brine with small amount of S6.

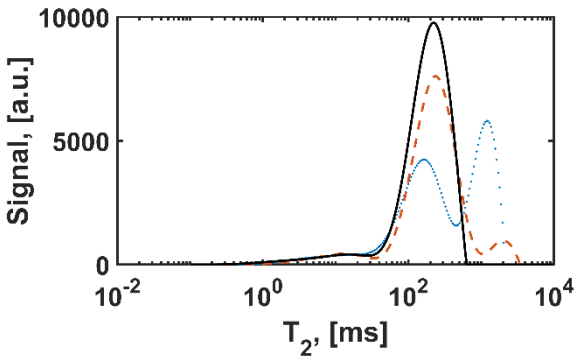

Fig. 7. ^{1}H bulk T_2 distribution for treated Bentheimer core plug initially saturated with S6 and flooded with brine. (——) corresponds to the initial state (fully oil saturated) and (---) is after 5 cc of brine injection. (…) is after 10 PV injection of brine.

3.2.3 S6 saturated untreated core plug with irreducible brine (Sample # C4 flooded with S6)

Figure 8 shows ^{13}C 1D images of the untreated Bentheimer core plug at multiple time points during flooding. Initially the sample was fully saturated with brine. As expected, the ^{13}C image at the initial time point revealed no signal. S6 was then injected and at three time points during the injection ^{13}C profiles were acquired. At

the time point where 1/2 PV was injected, a sharp front was observed. After 10 PV of S6 injection, the ^{13}C saturation is steady from the inlet up to the middle of the core plug, which means the hydrocarbon saturation is lower at the outlet. Since the core plug is water wet and brine was initially saturating the sample, we conclude that this region has a capillary end effect.

After 10 PV oil injection from the left side, the oil saturation was 85% in the first half of the core plug, which means the irreducible brine saturation was 15%. On the right side of the core plug the irreducible brine saturation was between 35-40 percent which is due to capillary end effects.

For bulk measurements of this sample, there was no reference condition of 100% oil saturation because the sample was initially saturated with brine. So, g/signal of core plug C3 was used as the reference. The mass of brine inside the fully saturated brine sample was converted to the equivalent volume of the S6 oil. The signal amplitude was 22.6 a.u. after one half PV oil injection. Comparing this value with the calibration sample and converted volume of oil, results in 1.54 gr of S6 which means oil saturation was 22.5 %. The signal amplitude was 74.9 a.u. after 10 PV oil injection. Comparing this value with the calibration sample and converted volume of oil, results in 5.82 gr of S6 which means oil saturation was 74.7 %. These oil saturation values are in close agreement with the saturations obtained from ^{13}C profiles.

As shown in Figure 6, and Figure 7, ^{1}H MR measurement cannot distinguish the two phases and no information regarding capillary end effects is obtained.

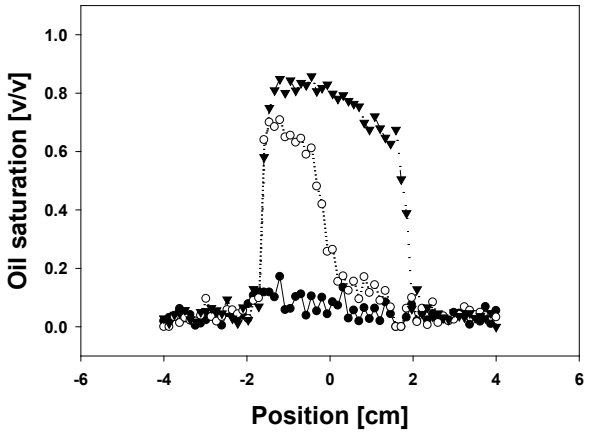

Fig. 8. ^{13}C Hybrid SE-SPI saturation profiles for untreated Bentheimer initially saturated with brine, flooded with S6. • is for the case of fully brine saturated sample inside the low pressure core holder when a small amount (less than 1 cc) of S6 was injected from left side. ○ is related to half PV of S6 injection. ▼ is related to 10 PV S6 injection.

^{1}H T_2 relaxation and profile measurements could not distinguish the two phases for this sample. Small differences in the signal are apparent, but T_2 mapping has overlapping components from which we conclude that using conventional ^{1}H profile measurements it was not possible to separate the two phases and calculate saturation of the fluids.

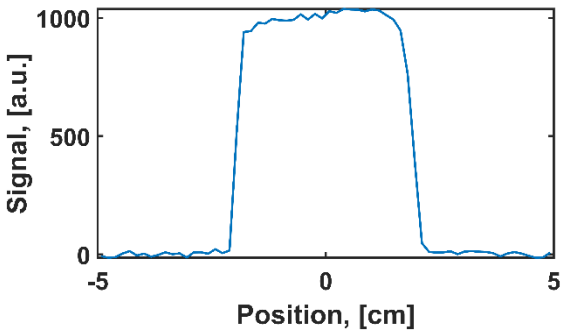

Fig. 9. ^{1}H T_2 mapping SE-SPI profile for untreated Bentheimer initially saturated with brine, flooded with S6.

As can be seen from Figure 10, signals from oil and water phases are not separable in the bulk T_2 distribution.

Comparing Figure 5 and Figure 8, it is observed that when the non-wetting phase was injected, there were two regions containing non-wetting phase. The first region has a piston like front moving with high saturation. There is also a region with low saturation at the front. But in the case in which the wetting phase was injected there was no clear distinction between these two limits and saturation dropped continuously from highest point (injection site) to the front location.

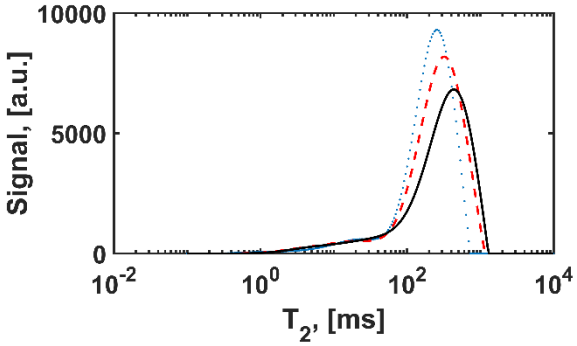

Fig. 10. ^{1}H bulk T_2 distribution for treated Bentheimer core plug initially saturated with brine and flooded with S6. (…) corresponds to the initial state and (---) is after one half PV of S6 injection. (▁) is after 10 PV injection of S6.

3.3. Coreflooding monitoring

A coreflooding experiment (drainage) was performed on Bentheimer and Berea core plugs. Figure 11 and Figure 12 show the saturation images based on ^{13}C MRI during the coreflooding experiment on the Bentheimer and the Berea core plugs respectively. Acquisition of each profile took 25 minutes. The measurement time is lengthy due to the long T_1 of the S20 oil and a higher number of scans was used for the measurements. Initially the samples were fully brine saturated and the S20 oil was injected from the left side of the core plugs. As can be seen initially no ^{13}C signal was observed, but after injection the observed oil saturation increases. After 5 hours of injection for the Bentheimer core plug and 8 hours of injection for the

Berea core plug, the shape of the profile was constant (steady state condition) and flow bumps were used to overcome the capillary pressure and reduce the irreducible water saturation. These increased flow rates are useful for relative permeability measurements by simulators. In the final state of injection, the oil saturation on the right side of the core plug is lower than the middle and left side of the core plug which is due to capillary end effects. After cessation of injection, the sample was removed from the core holder, and placed in the Dean-Stark apparatus for validation of the saturations.

In this paper we have considered various Bentheimer core plus (treated and untreated), and a single untreated Berea core plug, and the applicability of the ^{13}C Hybrid SE-SPI to obtain hydrocarbon profiles was confirmed. In the case of mixed-wet samples, if the relaxation times of the ^{13}C in different environments in the rock are close together then there will be no issue with ^{13}C Hybrid SE-SPI. If there is a range of T_2 lifetimes within the ^{13}C species, we have the possibility to discriminate them through ^{13}C T_2 mapping SE-SPI. Therefore, in that case ^{13}C T_2 mapping SE-SPI would be a good choice for hydrocarbon imaging. ^{13}C Hybrid SE-SPI is T_2 blurred which means a short T_2 lifetime may cause blurring. A short T_1 would not affect Hybrid SE-SPI, nor T_2 mapping SE-SPI. Each would be executed faster.

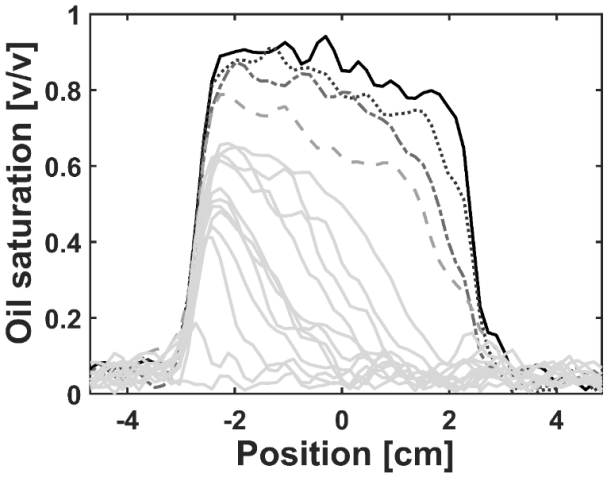

Fig. 11. Oil saturation profiles for the Bentheimer core plug F2. Flooding started with the rate of 0.015 ml/min and saturation profiles were continuously acquired. After 13 profiles, the flow rates increased stepwise. Each flow rate continued until a steady state condition was achieved. Light solid lines are related to the flow rate of 0.015 cc/min. They are followed by flow rates of 0.05, 0.1, 0.5 and 1 cc/min.

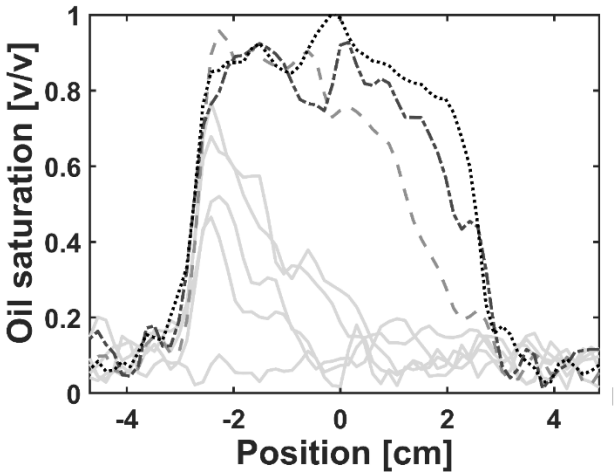

Fig. 12. Oil saturation profiles for the Berea core plug F1. Flooding started with the rate of 0.015 ml/min and saturation profiles were acquired at multiple time points. After 5 profiles, the flow rates increased stepwise. Each flow rate continued until a steady state condition was achieved. Light solid lines are related to the flow rate of 0.015 cc/min. They are followed by flow rates of 0.05, 0.1 and 0.5 cc/min.

3.4. Validation

To validate the profiles obtained by ^{13}C MRI, the average saturation obtained by the calibrated saturation profiles was compared with Dean-Stark measurement and the calibrated signal of the bulk CPMG. The average oil saturation based on ^{13}C MRI was 81.6 %. The average oil saturation based on ^{13}C MR (CPMG) was 77.7 %. The Dean-Stark experiment gave a water saturation of 18.1 ± 0.7 % which results in an oil saturation of 81.9 ± 0.7 %. This confirms the accuracy of the ^{13}C measurements. For this calculation ^{1}H MR measurement was used to calculate the total ^{1}H signal of the saturating fluids and by having the hydrogen index of the fluids (HI of S20 was 1.06), the pore volume was calculated. The pore volume derived with this method was consistent with gravimetric measurements. Water and oil saturations have also been confirmed with other methods (volumetric and gravimetric), with results that are not reported here.

4 Conclusion

Spatial determination of saturation requires methods that can differentiate the phases inside the porous medium. In this paper, ^{13}C measurements were used to isolate signal from hydrocarbons in the samples. This method enables us to obtain hydrocarbon profiles and saturations without the need to distinguish phases by relaxation times. Application of this measurement will assist in reliable analyses, not only in conventional crude oil, but also in heavy oil with very complex MR relaxation time distributions that prevent signal differentiation.

In this paper, ^{13}C MR measurements were used to obtain hydrocarbon saturation profiles in representative core plugs. The results clearly show capillary end effects

for both water wet and oil wet samples. The saturation profiles reveal invaluable information regarding residual/irreducible saturation of wetting/non-wetting phases. Moreover, we showed that ^{13}C MRI is reliable for saturation monitoring during coreflooding experiments with realistic parameters and with acceptable accuracy.

This method opens a new door for accurate saturation measurements and capillary end effect analysis which are used in enhanced oil recovery processes and relative permeability measurements.

These studies will be greatly facilitated by a variable field magnet which permits sequential measurement of ^{1}H and ^{13}C in the same magnet with the same RF probe. The ability of a variable field magnet to switch between monitoring ^{1}H and ^{13}C is critical to a comprehensive understanding of sample behavior.

^{23}Na MR/MRI measurement can also reveal valuable information regarding saturation profiles in coreflooding experiments. Since ^{23}Na is in the brine, there is similarly no need for discriminating relaxation times. This is a topic of interest for future work.

This work was supported by an NSERC Alliance award grant [ALLRP 571885–21] and an NSERC Discovery grant [2022-04003]. The authors thank TotalEnergies and Green Imaging Technologies for financial support.

References

[1] D.P. Green, J. Gardner, B.J. Balcom, M.J. McAloon, P.F. de J. Cano-Barrita (Eds.), Comparison Study of Capillary Pressure Curves Obtained Using Traditional Centrifuge and Magnetic Resonance Imaging Techniques, SPE, 2008.

[2] M. Li, L. Romero-Zerón, F. Marica, B.J. Balcom, Polymer Flooding Enhanced Oil Recovery Evaluated with Magnetic Resonance Imaging and Relaxation Time Measurements, Energy & Fuels 31 (2017) 4904–4914. https://doi.org/10.1021/acs.energyfuels.7b00030.

[3] M. Li, S. Vashaee, L. Romero-Zerón, F. Marica, B.J. Balcom, A Magnetic Resonance Study of Low Salinity Waterflooding for Enhanced Oil Recovery, Energy & Fuels 31 (2017) 10802–10811. https://doi.org/10.1021/acs.energyfuels.7b02166.

[4] N. Loahardjo, N.R. Morrow, J. Stevens, J. Howard, Nuclear magnetic resonance imaging: application to determination of saturation changes in a sandstone core by sequential waterflooding, SCA, Halifax (2010).

[5] Y. Zhao, Y. Zhang, X. Lei, Y. Zhang, Y. Song, CO2 flooding enhanced oil recovery evaluated using magnetic resonance imaging technique, Energy 203 (2020) 117878. https://doi.org/10.1016/j.energy.2020.117878.

[6] Q. Chen, B.J. Balcom, Measurement of rock-core capillary pressure curves using a single-speed centrifuge and one-dimensional magnetic-resonance imaging, J. Chem. Phys. 122 (2005). https://doi.org/10.1063/1.1924547.

[7] J. Mitchell, A.M. Howe, A. Clarke, Real-time oil-saturation monitoring in rock cores with low-field NMR, J. Magn. Reson. 256 (2015) 34–42. https://doi.org/10.1016/j.jmr.2015.04.011.

[8] J. Mitchell, E.J. Fordham, Contributed review: nuclear magnetic resonance core analysis at 0.3 T, Rev. Sci. Instrum. 85 (2014) 111502. https://doi.org/10.1063/1.4902093.

[9] M.J. Dick, D. Veselinovic, D. Green, Spatially resolved wettability measurements using nmr wettability index, E3S Web Conf. 89 (2019) 3001. https://doi.org/10.1051/e3sconf/20198903001.

[10] C.E. Muir, B.J. Balcom, A comparison of magnetic resonance imaging methods for fluid content imaging in porous media, Magnetic Resonance in Chemistry 51 (2013) 321–327. https://doi.org/10.1002/mrc.3947.

[11] D. Olsen, S. Topp, A. Stensgaard, J.V. Nørgaard, J. Reffstrup, Quantitative 1D saturation profiles on chalk by NMR, Magnetic Resonance Imaging 14 (1996) 847–851. https://doi.org/10.1016/S0730-725X(96)00214-7.

[12] M. Rauschhuber, G. Hirasaki, Determination of saturation profiles via low-field NMR imaging, SCA, Noordwijk (2009).

[13] P. Yang, H. Guo, D. Yang, Determination of Residual Oil Distribution during Waterflooding in Tight Oil Formations with NMR Relaxometry Measurements, Energy Fuels 27 (2013) 5750–5756. https://doi.org/10.1021/ef400631h.

[14] S. Vashaee, M. Li, B. Newling, B. MacMillan, F. Marica, H.T. Kwak, J. Gao, A.M. Al-harbi, B.J. Balcom, Local T1-T2 distribution measurements in porous media, J. Magn. Reson. 287 (2018) 113–122. https://doi.org/10.1016/j.jmr.2018.01.001.

[15] Florin Marica, Armin Afrough, Derrick Green, Laura Romero-Zeron, Bruce Balcom, Direct Magnetic Resonance Measurement of Average Pore Size, SCA, Pau (2019).

[16] R. Gupta, D.R. Maloney, Intercept Method—A Novel Technique To Correct Steady-State Relative Permeability Data for Capillary End Effects, SPE Res Eval & Eng 19 (2016) 316–330. https://doi.org/10.2118/171797-PA.

[17] D.D. Huang, M.M. Honarpour, Capillary end effects in coreflood calculations, Journal of Petroleum Science and Engineering 19 (1998) 103–117.

[18] L.B. Romero-Zeron, The role of porous media wettability on foamed gel propagation and fluid diverting performance. Ph.D, University of Calgary (Canada), 2005.

[19] L. Li, Q. Chen, A.E. Marble, L. Romero-Zerón, B. Newling, B.J. Balcom, Flow imaging of fluids in porous media by magnetization prepared centric-scan SPRITE, J. Magn. Reson. 197 (2009) 1–8. https://doi.org/10.1016/j.jmr.2008.10.020.

[20] N. Ansaribaranghar, L. Romero-Zerón, F. Marica, B.J. Balcom, Measurement of crude oil emulsion instability using magnetic resonance and magnetic resonance imaging, Colloids and Surfaces A: Physicochemical and Engineering Aspects 666

(2023) 131330. https://doi.org/10.1016/j.colsurfa.2023.131330.
[21] L. Li, H. Han, B.J. Balcom, Spin echo SPI methods for quantitative analysis of fluids in porous media, J. Magn. Reson. 198 (2009) 252–260. https://doi.org/10.1016/j.jmr.2009.03.002.
[22] O.V. Petrov, G. Ersland, B.J. Balcom, T_2 distribution mapping profiles with phase-encode MRI, J. Magn. Reson. 209 (2011) 39–46. https://doi.org/10.1016/j.jmr.2010.12.006.
[23] J. Mitchell, J. Staniland, R. Chassagne, E.J. Fordham, Quantitative In Situ Enhanced Oil Recovery Monitoring Using Nuclear Magnetic Resonance, Transp Porous Med 94 (2012) 683–706. https://doi.org/10.1007/s11242-012-0019-8.